

15.4.85

46

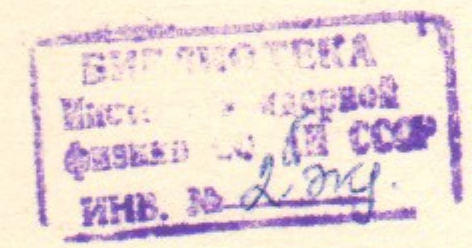
№ 92
1985



ИНСТИТУТ ЯДЕРНОЙ ФИЗИКИ СО АН СССР

V.M. Aulchenko, A.G. Chilingarov,
A.N. Krinitsyn, L.M. Kurdadze, M.Yu. Lelchuk,
V.P. Nagaslaev, L.V. Romanov

MYLAR DRIFT TUBES FOR TRACKING



PREPRINT 84-166



НОВОСИБИРСК

V.M. Aulchenko, A.G. Chilingarov,
A.N. Krinitsyn, L.M. Kurdadze, M.Yu. Lelchuk,
V.P. Nagaslaev, L.V. Romanov

Mylar Drift Tubes for Tracking

ABSTRACT

A technology of manufacturing aluminized mylar tubes with wall thickness of 20 micron has been developed. Using a hodoscope of 16 drift tubes the 80 micron resolution for minimum ionizing particles has been obtained.

This work presents the results of testing a hodoscope coordinate system for charged particle tracking. The design of the hodoscope is based on a tube with 20 micron thick walls manufactured from aluminized mylar.

The obvious advantages of tube hodoscope systems (drift, streamer, etc.) provided their fruitful applications in shower and range parts of modern detectors both in colliding beam and fixed target experiments [1, 2]. Metal or plastic tubes are usually employed. The wall thickness is not very important.

To use drift tubes for tracking, however, their walls should be thin enough so that contributions of the wall material and gas to a multiple scattering be comparable. Mylar tubes allow the application of hodoscopes instead of traditional multiwire drift chambers in tracking parts of detectors, since mylar does not bring more material than cathode wires.

The similarity of hodoscope elements is particularly suited to series production and facilitates system calibrations. The independence of separate elements diminishes cross-talks and provides the high reliability of the system. Any malfunctioning tube may be separately disconnected without affecting overall operation of the system.

Besides that, due to a large cathode surface drift tubes would be less affected by ageing processes compared to the chambers with cathode wires [3, 4]. In a cylindrical tube the electric field is axially symmetric in a whole sensitive volume. Therefore isochrones (lines with an equal drift time) are circles even in the case of the magnetic field, thereby substantially facilitating track reconstruction.

The development of coordinate systems with mylar tubes started in the Novosibirsk Institute of Nuclear Physics in connection with a design of a new detector for colliding beams. The first hodoscope consis-

ting of 7 mylar tubes with 28 mm diameter was constructed in 1982 [5]. With a mixture of Ar + 10%CO₂ the spatial resolution of 220 micron was obtained. The resolution value was limited by an inaccuracy of mechanical assembling of the hodoscope as well as by an inaccuracy of drift characteristics.

Hodoscope coordinate systems (vertex detectors) with mylar tubes were independently studied at SLAC [6, 7]. These tubes were commercially manufactured, using the technology differing from that described here. The wall thickness of tubes manufactured for HRS and MAC detectors is 4–5 times greater than that in our tubes.

1. Drift tube and hodoscope structure. In the designed hodoscope system the small size cell has been chosen, the tube diameter being 14 mm. The drift tube structure is shown in Fig. 1. It consists of a mylar cathode, two plugs and an anode wire. The cathode is made of a wide aluminized mylar leaf 20 micron thick. The thickness of aluminum coating is about 0.03–0.07 micron. The surface resistivity of the aluminum coating is 0.4–0.8 Ohms per square.

Mylar tubes were constructed at the special tool using ultrasonic welding (Fig. 2). One mylar layer was wound on a smooth steel tube of diameter 14 mm. Mylar was kept at the tube surface due to air suction through thin holes in its wall. The titanium head of a wave-guide transmitting mechanical ultrasonic vibrations from a nickel magnetostrictive converter was pressed against the mylar surface. The converter was excited by an ultrasonic frequency generator USG-3-0,4 with a power up to 400 W. The wave-guide head was moved by an electric driver at a constant speed from one end of the tube to another welding a mylar cylinder along its generatrix. The resulting weld width did not exceed 1 mm, an overlap width being less than 2 mm. The resulting tube was cut off from the mylar leaf. The appropriate wave-guide shape and welding regime provided good weld quality, leak-proofness of the tube and good cylindricity in the weld region.

Because of the different size and shape of the plugs at tube ends, the prepared tube could be inserted or removed from the hodoscope through one of the end plates (Fig. 1). The plug consisted of inner and outer brass details separated by an insulator of organic glass. The high accuracy of the outer fitting surfaces of the plugs ensured fine fixation of the tube at the hodoscope endplates. A 1.5 mm hole in the plug centre served both for accomodating an anode wire at the place of soldering and flowing operational gas through the tube. The tag for connection with electric circuits was soldered to the plug before tube assembling.

After the mylar cylinder had been glued to the plugs, the anode wire was drawn through the tube and strung. Tube plugs fixed in a separate device, an anode wire was installed at the centre of plug fitting surfaces and soldered as shown in Fig. 1. We checked that after cooling of a solder drop the wire shifted by less than few a micron.

The 18 micron diameter gold-plated tungsten wires with 800 Ohm/m resistance were used as anode wires. They were tensioned to 60 g. The assembled tube is mechanically stable and can be easily moved to the hodoscope.

Before being installed in a hodoscope, the prepared tubes were blown through by the operational gas mixture and tested at the separate stand. The gas gain homogeneity along the wire was tested and the HV width of an efficiency plateau was determined.

16 mm thick aluminum endplates are held apart by studs forming a hodoscope frame. Fine positioned fit holes were drilled in the plates. The prepared tube was drawn through the larger hole (from the left to the right in Fig. 1) and then slightly stretched from the other side by a nut with a calibrated spring.

Drift tube characteristics were studied using the test hodoscope of 16 tubes. The general lay-out of the hodoscope is shown in Fig. 3. The mylar tube length was 40 cm. First results were obtained in mixtures of argon with 10%, 30%, 50% of carbon dioxide and 30% of isobutane at atmospheric pressure. The gas was mixed in a flow. The flow rate was about 2 hodoscope volumes per hour (0.5 cm³/sec). Before mixing carbon dioxide was passed through the purifying system where silica aerogel and activated carbon absorbed organic impurities. To avoid the diffusion of atmospheric gases and, in particular, water vapour through a thin mylar wall into the operational volume, the hodoscope was placed in a common mylar bag (Fig. 6) which was also blown through by the operational mixture. After the hodoscope assembling the stability of drift tubes operation was checked with ⁵⁵Fe and ⁹⁰Sr sources. The tube was light sensitive since photoelectrons were knocked out from the thin aluminum cathode due to photoeffect. Single electron signals turned out to be useful for gas gain calibrations.

2. Electronics provides measurements of a transverse coordinate by the drift time and a longitudinal one by the charge division.

The electronics circuit with the exception of CAMAC units is shown in Fig. 4. Signals from both wire ends are transmitted through blocking capacitors and 1.2 m cables to preamplifiers. The preamplifiers (PA) has a gain about 130 and a bandwidth of 7 MHz. An input resistance is equal to 75 Ohms.

The amplified signals are transmitted to differential drivers (DD) through twisted pairs. After that the signals are branched and transmitted to integrators (I) and a summator (S). After the integrator the signals are proportional to the input charge. These signals are differentiated with delay lines. Through invertors (Inv) and followers the signals are finally transmitted to the output. As a result the pulse height $A1$ and $A2$ are proportional to the charges from the wire ends.

From the summator a sum of the signals is transmitted to the discriminator (D), which produces a time mark (T) defining a drift time. The discriminator threshold was set to 10^{-14} Coulomb providing a hit from a single electron at the available gas gain.

The $A1$, $A2$ and T signals are transmitted to an analog memory (AM) and a time-to-amplitude converter (TAC) both in CAMAC (Fig. 5). The special unit (amplitude-to-digit converter and memory, ADC&M) reads the information from the AM and the TAC and digitizes received data with the 10-bit ADC. After the subtraction of pedestals stored in the ADC&M the data are recorded in the memory of the ADC&M and read out by a computer. A single ADC&M can read 8 TAC or AM units.

3. Spatial resolution of the drift tubes was measured with cosmic ray particles. The hodoscope was triggered using three-fold coincidence of the signals from the scintillation counters (Fig. 6). To decrease a background due to the photoemission from the cathode surface the hodoscope was screened from the light. The information about events was recorded on the magnetic tape.

The operational voltage depends on gas mixture. At the discriminator threshold of 10^{-14} coulomb it equals 1640 V for the Ar-CO₂ (90:10) and 2320 V for Ar-CO₂ (50:50). At the operational voltage the efficiency is greater than 99%. For mixtures containing CO₂ a plateau is greater than 100 V while for the mixture with the iC₄H₁₀ it is greater than 300 V.

The time-distance relationship was measured using two methods. In the first one a drift velocity was measured in a uniform electric field. A value of this field could be varied from 100 V/cm to 3500 V/cm.

In the second one the time-distance relationship was obtained from the drift time distribution for one tube. If the tube is uniformly irradiated the drift time distribution is proportional to the drift velocity:

$$\frac{dN}{dt} = \frac{dN}{dr} \cdot \frac{dr(t)}{dt} = \frac{1}{r_0} v(t);$$

where $r_0 = 1/(dN/dr)$ is equal to the maximum drift distance. Integrating over the drift time distribution one can determine the time-distance relationship (Fig. 7)

$$r(t) = r_0 \frac{N(t' < t)}{N_{total}}$$

This time-distance relationship automatically takes into account a finite spacing of the primary ionization clusters along the track. For the used gas mixtures the average distance d between the clusters is about 0.3 mm (at the atmospheric pressure). If a distance between the wire and the track is sufficiently big, some clusters arrive to the wire simultaneously and the cluster structure of the track can be neglected. If the track goes just through the wire, an average drift time corresponds to $d/2$ rather than zero. As a result the time-distance relationship deviates from a straight line at small r .

For the determination of the final time-distance relationship results obtained by both methods were taken into account. Examples of the final time-distance relationships are shown in Fig. 8. These time-distance relationships were used for tracking.

For data processing events with 4 hit tubes were selected. An optimum straight line was obtained by fitting drift radii measured in

these tubes. After that a value $S = \sum_{i=1}^4 (r_i - r_i^p)^2$ was calculated, where r_i is a drift radius and r_i^p is a perpendicular from the tube centre to the track. As 2 parameters (the arrival point and the azimuthal angle of the particle) were fitted, the S distribution is proportional to the χ^2 distribution with 2 degrees of freedom:

$$\frac{dN}{dS} \sim \exp\left(-\frac{S}{2\sigma^2}\right)$$

where σ is an average resolution of a single tube. This value can be calculated from a line slope fitted by the logarithmic S distribution.

The experimental S distribution (Fig. 9) is not completely described with one exponential curve. This phenomenon is very likely caused by the drift radius dependence of the spatial resolution. In Fig. 9 two lines are shown for both gas mixtures. Each line is fitted by the events set on the left side of the corresponding mark. For Ar-iC₄H₁₀ (70:30) (Fig. 9,a) the resolution equals 80 μm for 88% of events (line 1) and 90 μm for 95% of events (line 2). For Ar-CO₂ (50:50) (Fig. 9,b) the resolution is 80 μm for 80% of events (line 1) and 90 μm for 87% of events (line 2). If one diminishes the CO₂ concentration the resolution

deteriorates. This effect is likely caused by the diffusion of primary ionization. For Ar-CO₂ (70:30) the resolution is 110 μm for 82% of events. For Ar-CO₂ (90:10) the resolution is 140 μm for 85% of events.

The electronics contribution to this value because of noise, nonlinearities and instabilities is less than 50 μm for a run of 60–80 hours. Therefore the obtained resolution is mainly determined by the longitudinal diffusion of primary ionization and the inaccuracy of the time-distance relationship.

A possibility of measuring the longitudinal coordinate by the charge division was also checked. In the first measurements the resolution of 5 mm was obtained for cosmic particles. The wire length was equal to 500 mm.

At the present time work on improving both transverse and longitudinal resolution is in progress. The ageing of the tubes will be investigated. Then optimal gas mixtures will be chosen. But even existing results allow to begin construction of the large drift system consisting of drift mylar tubes.

In conclusion the author would like to thank V.I. Isachenko and V.D. Kutovenko for manufacturing and tuning the electronics and Y.V. Tenenev and A.V. Chegodaev for assistance in the experiments.

REFERENCES

1. G. Gidal et al. Preprint LBL-91/UC-37 (1983).
2. E. Iarocci. Proceedings of the International Conference on Instrumentation for Colliding Beam Physics. Stanford (1982).
3. G. Charpak et al. Nucl. Inst. Meth. 99 (1972) 279.
4. J. Adam et al. Nucl. Inst. Meth. 217 (1983) 291.
5. V.P. Nagaslaev. Graduation thesis. Novosibirsk University (1982).
6. D. Rust. Proceedings of the Third International Conference on Instrumentation for Colliding Beam Physics. Novosibirsk (1984).
7. E. Fernandez et al. Preprint SLAC-PUB-3390 (1984).

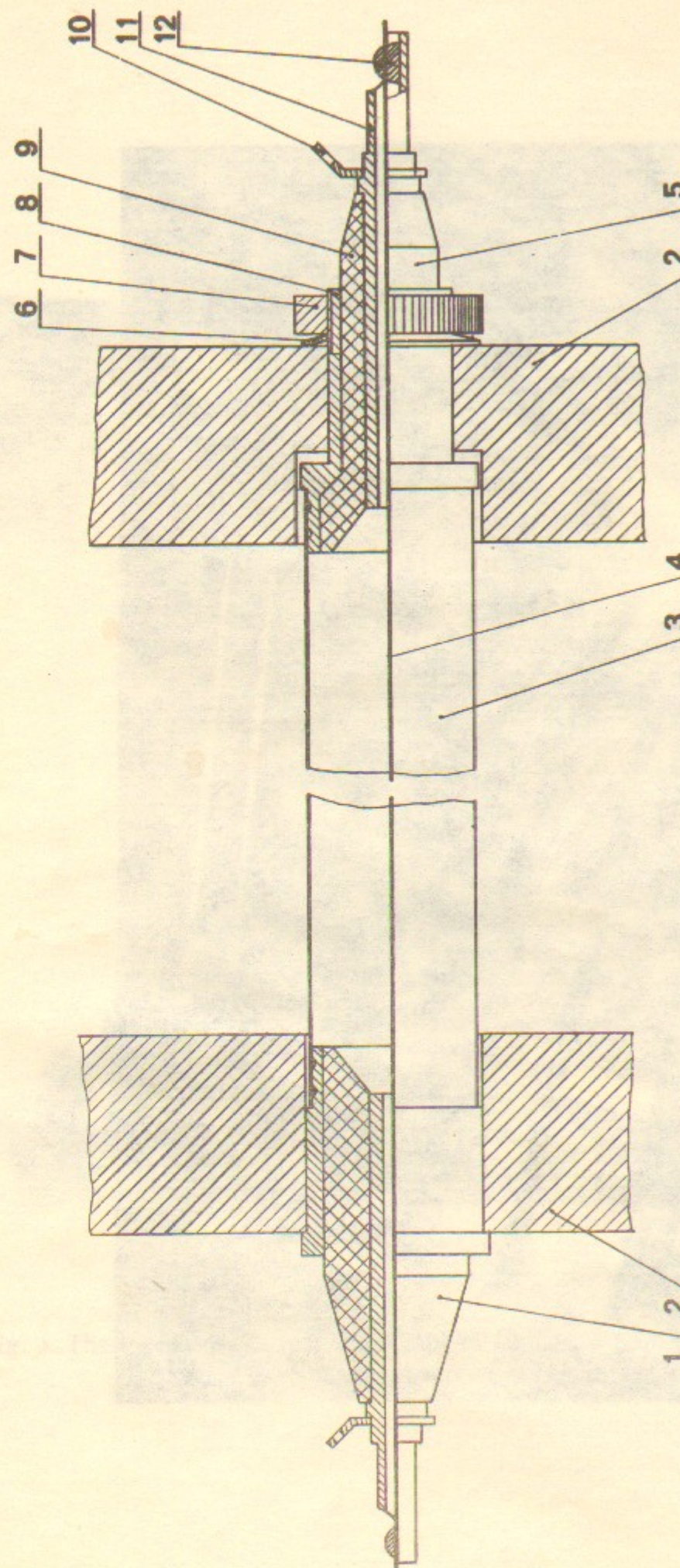


Fig. 1. The drift tube structure:

1—the larger plug; 2—the smaller plug; 3—the aluminumized mylar tube; 4—the anode wire; 5—the outer brass detail of a plug with a finely performed fitting surface; 6—the insulator; 7—the spring; 8—the nut; 9—the soldering tag electrically connected to the wire; 10—the inner brass detail of a plug; 11—the soldering place of the anode wire; 12—the soldering place of the anode wire.

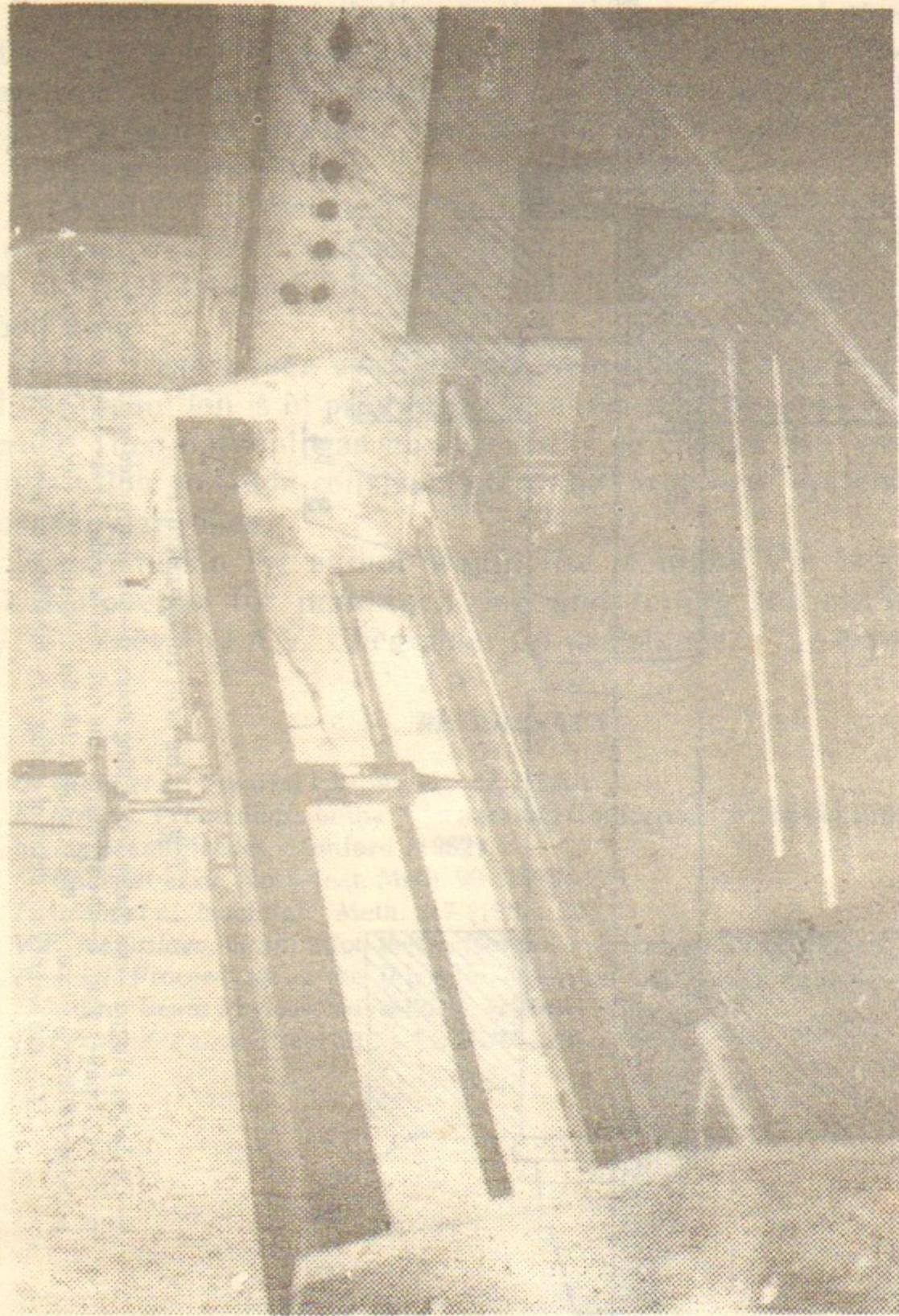


Fig. 2. The tool for ultrasonic welding of mylar tubes.

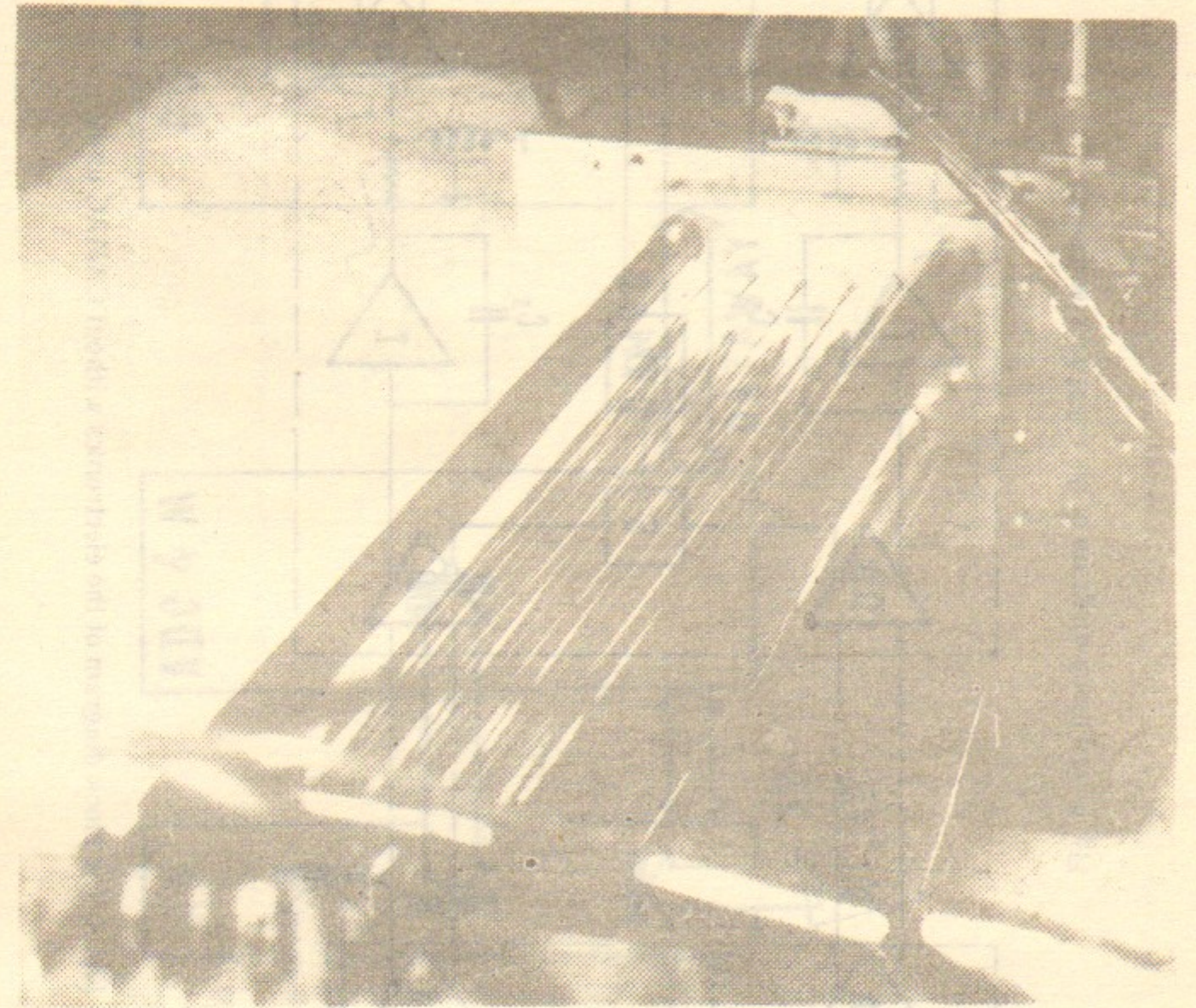


Fig. 3. The layout of the test hodoscope of 16 drift tubes. The gas preserving bag and the foil screen are removed.

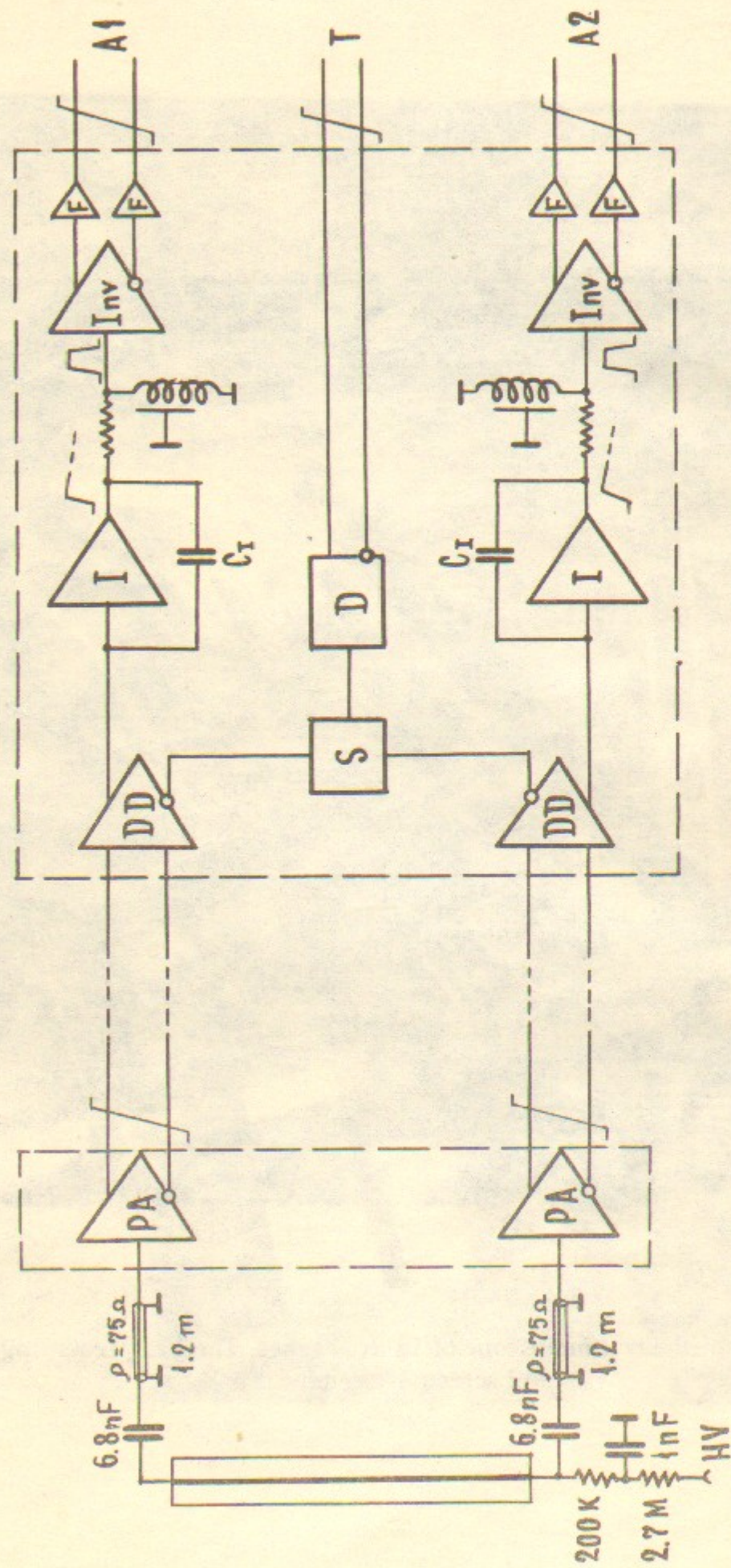


Fig. 4. The block diagram of the electronics without CAMAC units.

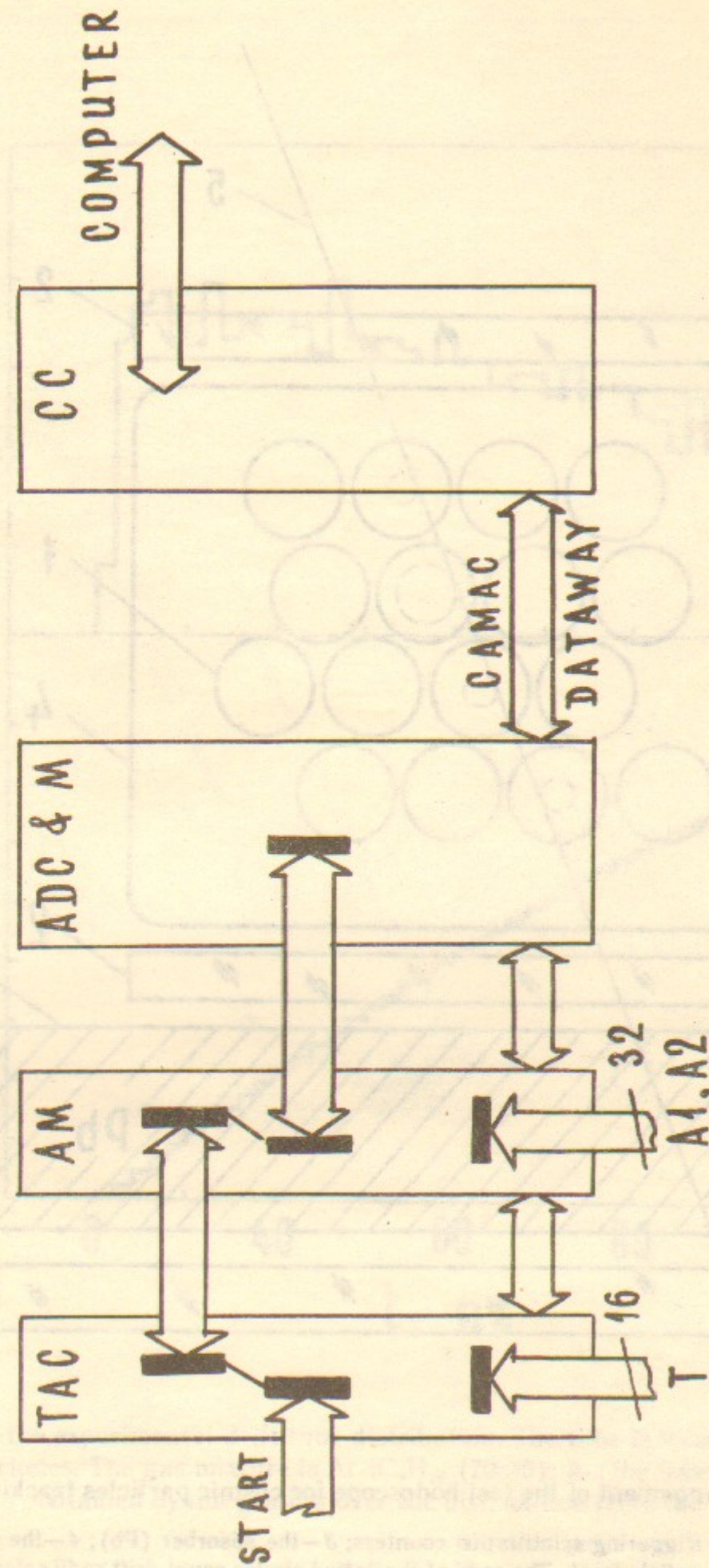


Fig. 5. The block diagram of the CAMAC electronics.

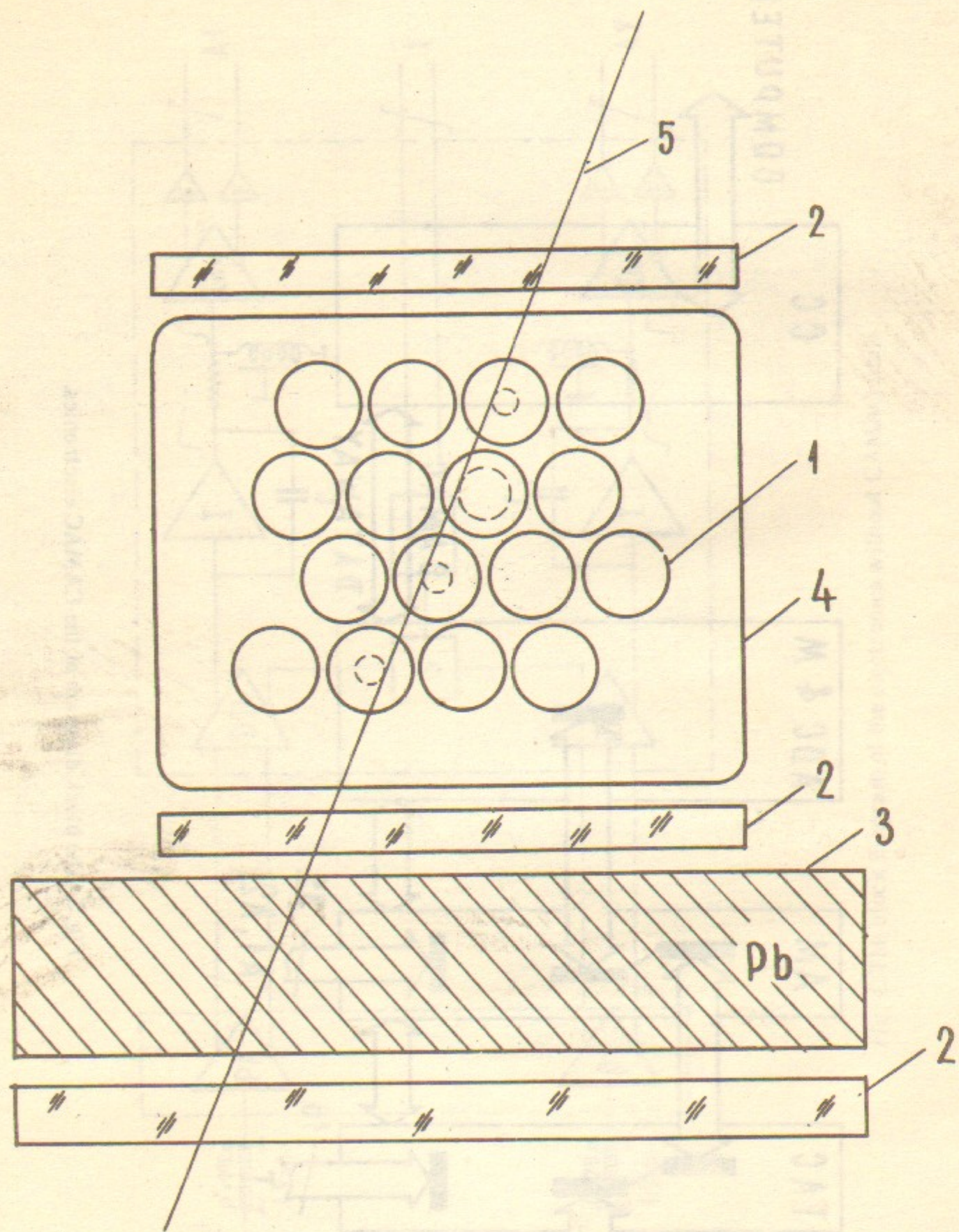


Fig. 6. The arrangement of the test hodoscope for cosmic particles tracking:

1—the drift tube; 2—the triggering scintillation counters; 3—the absorber (Pb); 4—the gas preserving bag; 5—the cosmic particle track. The radii of the dotted circles equal drift radii calculated from the drift times.

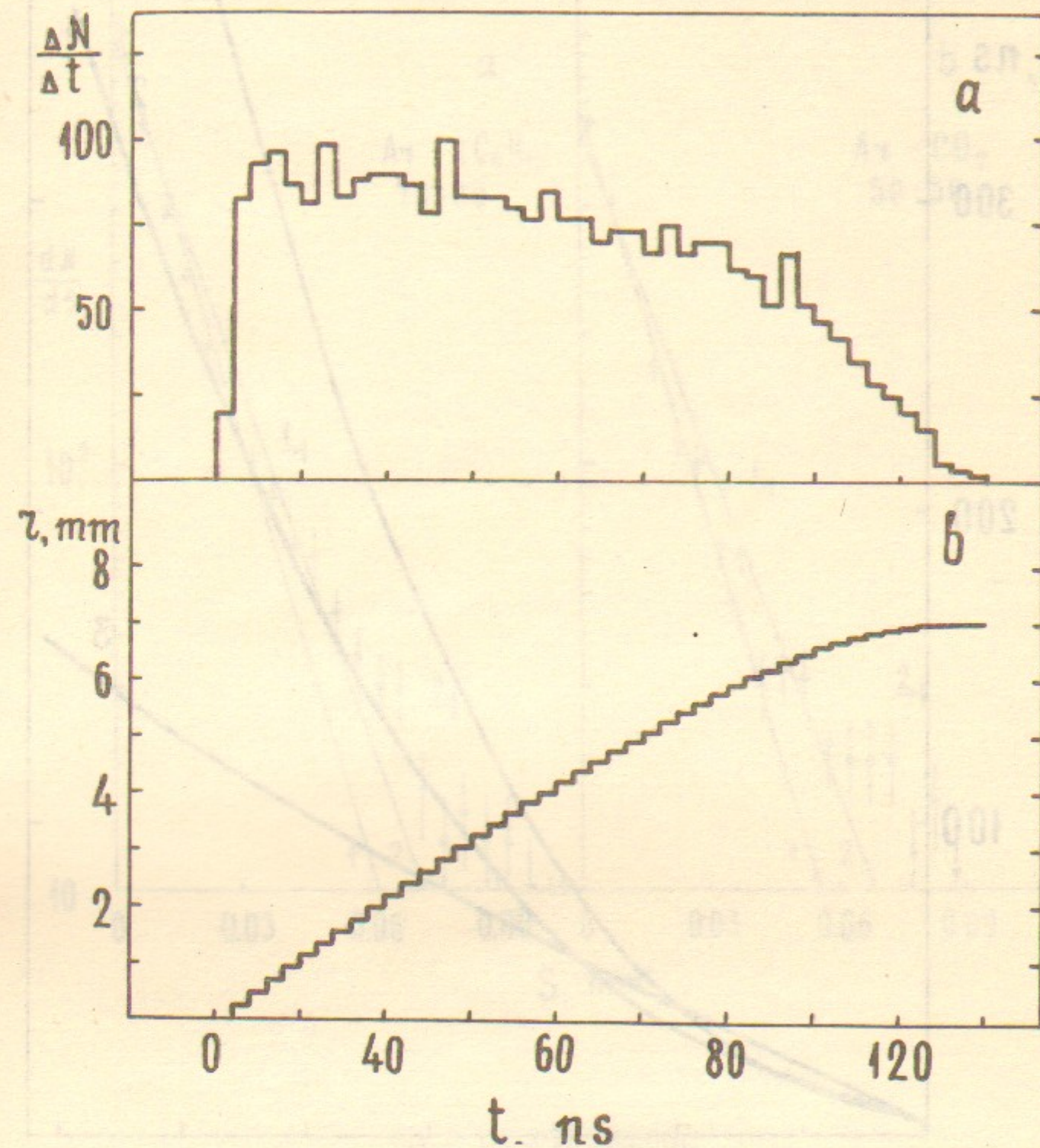


Fig. 7. a—the experimental drift time distribution. The tube is irradiated uniformly with cosmic particles. The gas mixture is Ar- iC_4H_{10} (70:30); b—the time-distance relationship obtained by integrating over the distribution from the Fig. 7, a.

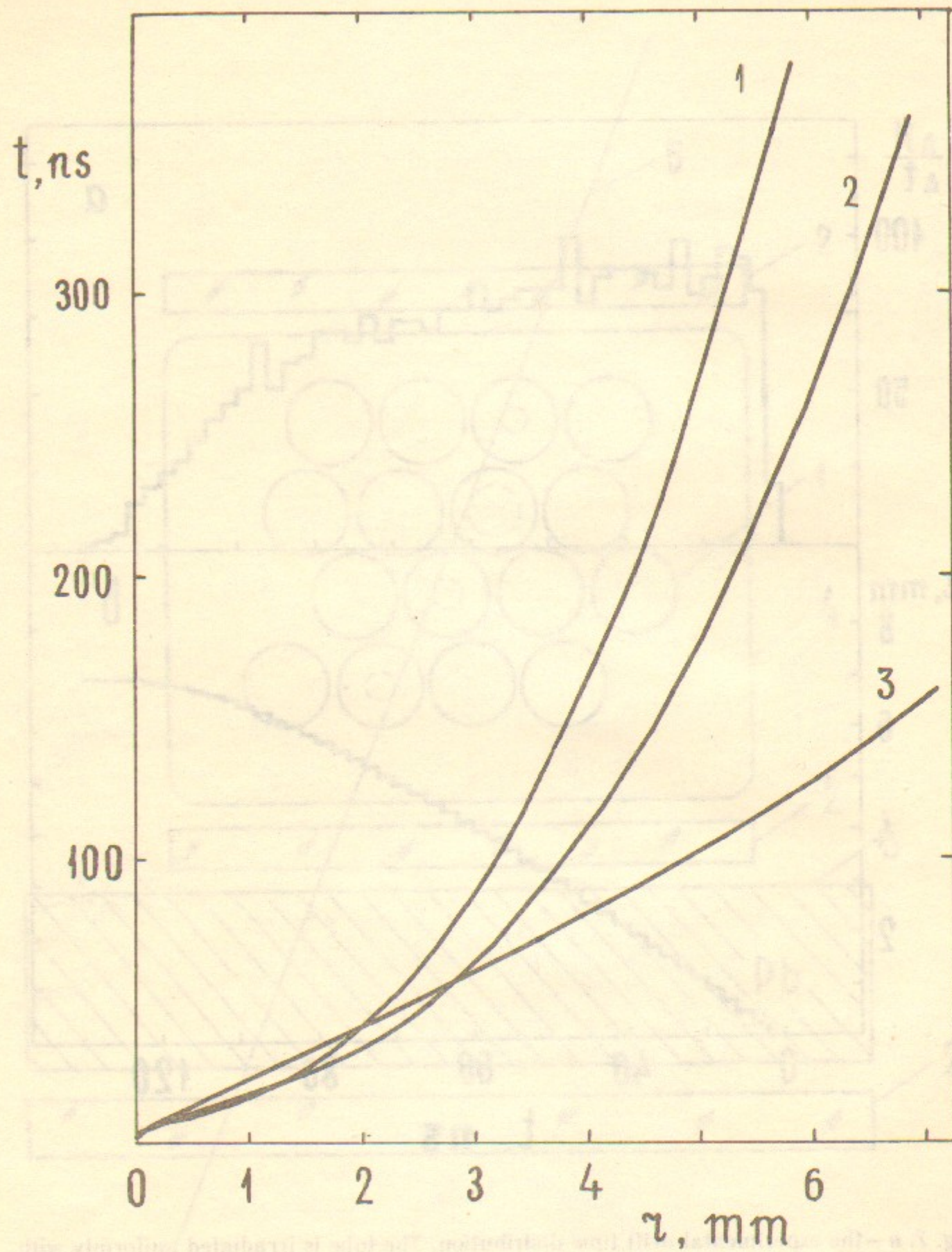


Fig. 8. The time-distance relationship for gas mixtures:
 1—Ar-CO₂ (50:30); 2—Ar-CO₂ (70:30); 3—Ar-iC₄H₁₀ (70:30).

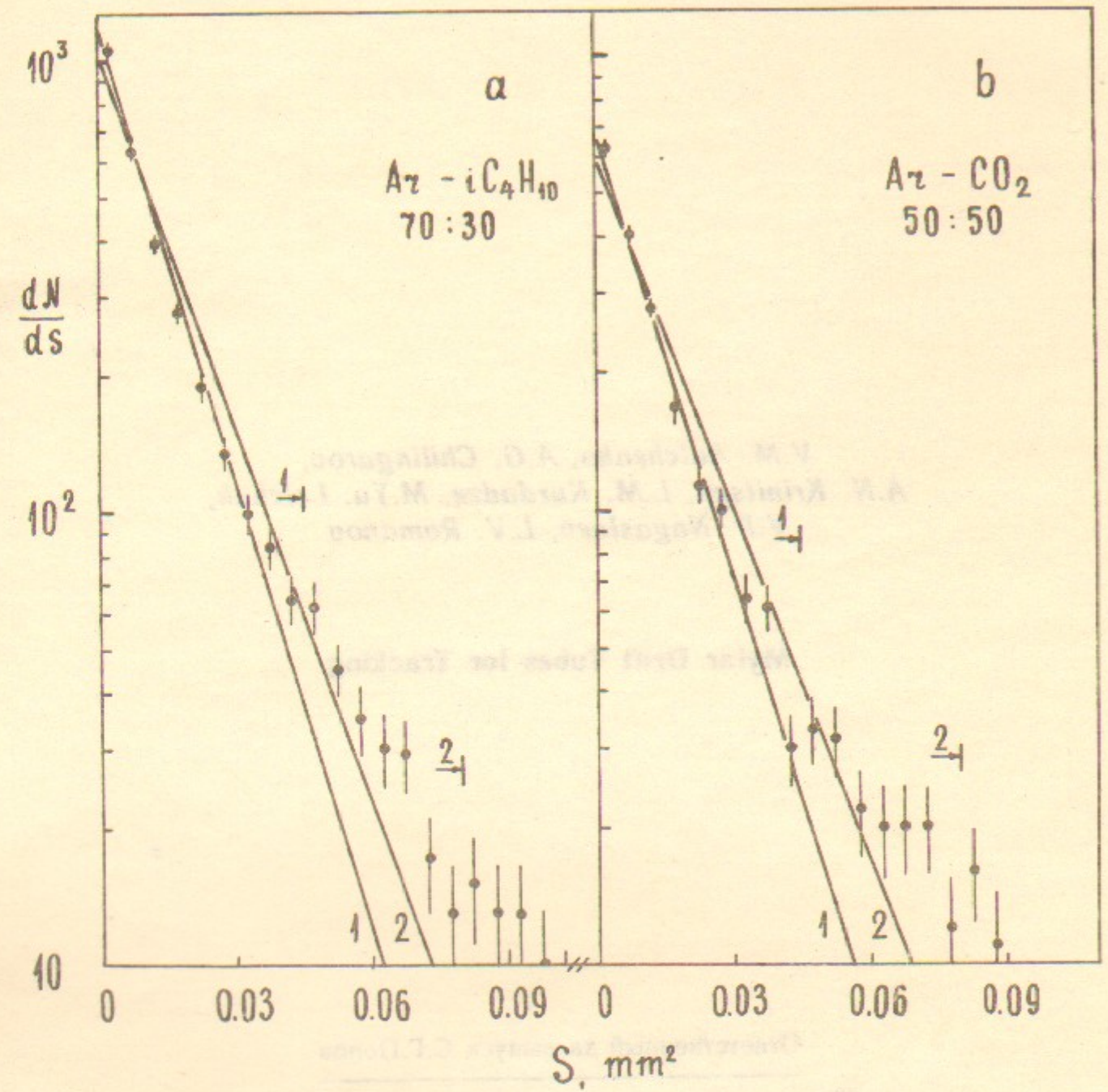
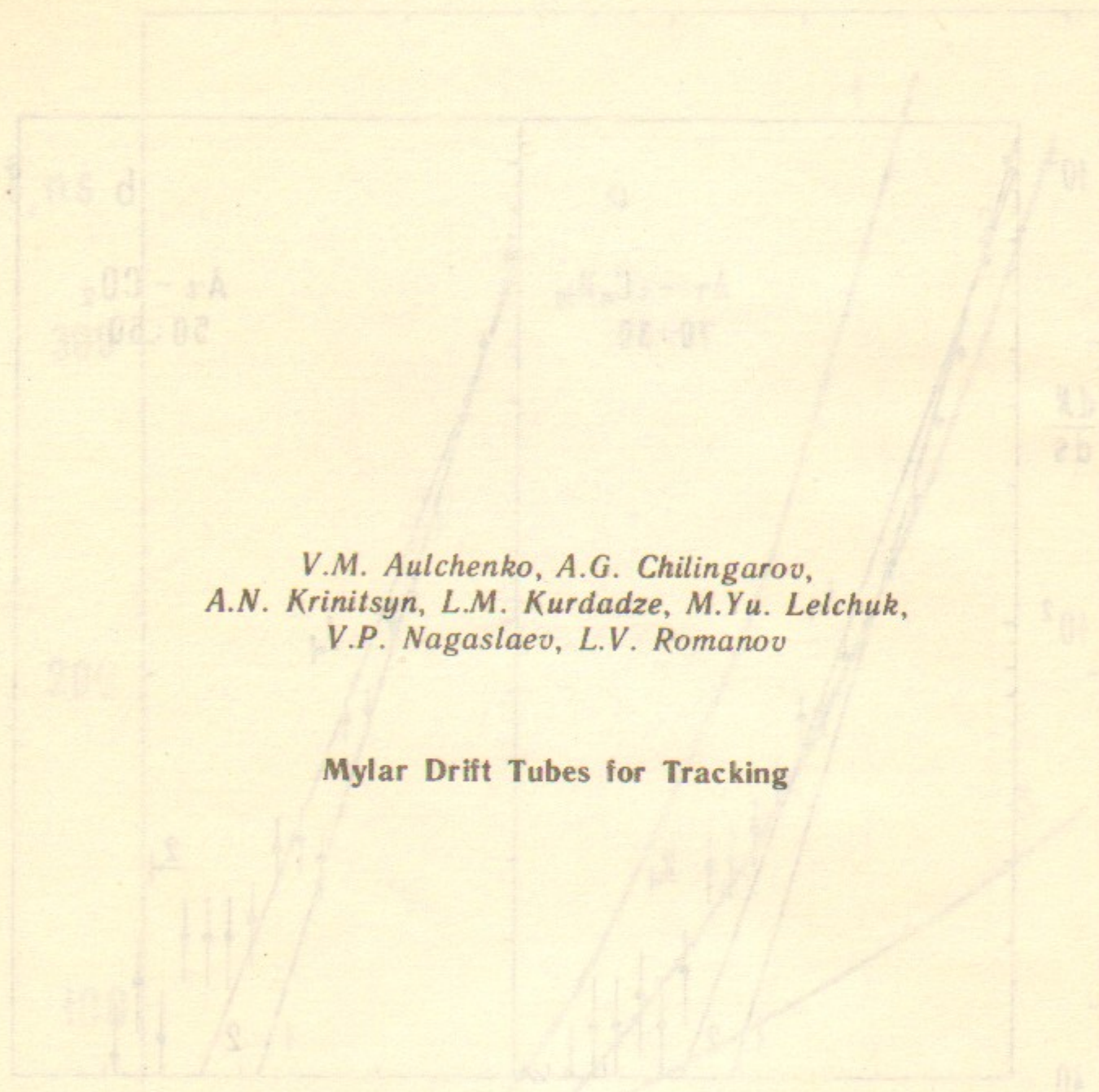


Fig. 9. The S-distribution:

a—for the Ar-iC₄H₁₀ (70:30) mixture. Line 1 is fitted by 88% of events set on the left side of the mark 1; line 2 is fitted by 95% of events set on the left side of the mark 2. b—for the Ar-CO₂ (50:50) mixture. Line 1 is fitted by 82% of events set on the left side of the mark 1; line 2 is fitted by 87% of events set on the left side of the mark 2. Lines 1 correspond to the resolution of 80 μm. Lines 2 correspond to the resolution of 90 μm.



*V.M. Aulchenko, A.G. Chilingarov,
A.N. Krinitsyn, L.M. Kurdadze, M.Yu. Lelchuk,
V.P. Nagaslaev, L.V. Romanov*

Mylar Drift Tubes for Tracking

Ответственный за выпуск С.Г.Попов

Подписано в печать 29.12 1984 г. МН 06545
Формат бумаги 60×90 1/16 Объем 1,5 печ.л., 1,2 уч.-изд.л.
Тираж 290 экз. Бесплатно. Заказ № 166

*Набрано в автоматизированной системе на базе фотона-
борного автомата ФА 1000 и ЭВМ «Электроника» и от-
печатано на ротапринтере Института ядерной физики СО
АН СССР,
Новосибирск, 630090, пр. академика Лаврентьева, 11.*